CHAPTER VI

THERMOLUMINESCENCE DATING

In this chapter, basic concept of dating paleoearthquake is revealed at the first section in order to provide the general concept of how to determine ages of paleoearthquakes. The second section is a brief review on Quaternary dating methods, and suitable materials used for dating methods are also summarized in this section. In addition, thermoluminescence(TL-) dating has explained in the third section which is composed of four subsections; basic concept of TL-dating, paleodose and annual dose evaluation, paleodose correction, and plateau test. Finally, TL-dating result of this thesis study is cited in the last section.

6.1 Dating Paleoearthquake

The main purpose of dating investigation in this thesis study is to determine bracketing age of past earthquakes or faulting events, especially prior to historical period or called paleoearthquakes. There are two methods for determining age of paleoearthquake; directly and indirectly. Direct dating is composed of two techniques which are scarp degradation modeling and age estimation from soil development on fault scarp techniques. These techniques are directly used to date the formation of coseismic scarp via scarp degradation modeling and quantitative analysis of scarp soils, respectively. However, large amount of age uncertainties is found in these techniques. In contrast, indirect methods have provided higher accuracy of numerical datings. The methods are involved age dating of fault-related sediments or landforms (McCalpin, 1996).

There are three techniques for indirect dating, namely, geomorphic, displaced deposit, and colluvial-wedge dating. In this thesis study, only displaced-deposit dating technique is applied due to faults that have been clearly observed cutting across sedimentary layers in the study area. According to this technique, the basic concept is mainly based on structural geology, which explains for the individual faulting event. Generally speaking, age of the event must be younger than faulted bed and older than the overlain unfaulted bed. For example, in Figure 6.1, there are units 1,2, and 3 found displaced by faults and overlain by units 4, 5, and 6. It can be explained that faulting event must be occurred between deposition of units 3 and 4.

6.2 Quaternary Dating Methods

After faults or other evidences of paleoearthquakes have been identified in the field, selected layers of fault-related sediments are proposed to carry out bracket age of faulting event as the following steps. To determine age of fault-related sediments, suitable methods of dating are chosen depending mainly on properties of materials and accuracy and precision of dating methods. Because it is important that different dating methods are become with different tasks and dated materials. For a past few decade, dating methods for Quaternary materials have been developed and applied to solve fault problems. Pierce (1986) had reviewed 18 dating methods and their datable materials for neotectonic studies as shown in Table 6.1. All these methods can be grouped into five types; annual, radiometric, radiogenic, process-oriented, and correlative. In the following year, Colman (1987) had grouped Quaternary dating methods into four main types; numerical age, calibration age, relative age, and correlation age. However, because it is beyond the scope of this study, further information for all methods is not described herein except radiogenic TL-dating due to its application in this thesis.

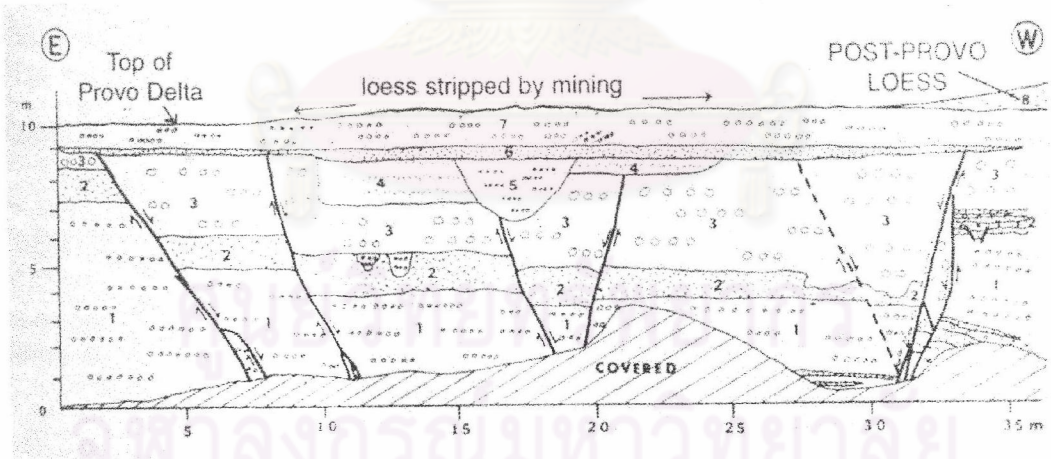

Figure 6.1. Trenching wall of a gravel pit showing normal faults cut across sedimentary layers. This faulting event must be occurred between depositions of units 3 and 4(after McCalpin, 1996).

Table 6.1. The summarization of dating methods for neotectonic studies (after Pierce, 1986).

	Dating method	Material dated
Annual	Historical records	Eye withness accounts, historical documents, legends
	Dendrochronology	Annual tree rings
	Varve chronology	Deformed lake sediments
Radiometric	Carbon-14	Charcoal, peat and shells from offset datum horizon
	Uranium-series	Fossil coral reefs, molluscs, bone, pedogenic carbonate
	Potassium-argon fission track	K-bearing igneous rocks, volcanic glass shards, zircon
Radiogenic	Uranium trend	Alluvium colluvium, loess
	*Thermoluminescence	Quartz and feldspar grains in fault scarp-derived colluvium
	Electron spin resonance	Quartz-bearing fault gouge
Process-oriented	Amino-acid racemization	Mollusca, skelatal material
	Lichenometry	Lichen on gracial morianes and fault scarps
	Soil chronology	Degree of soil development on offset geometric surfaces
	Rock weathering	Rock vanish, weathering rinds
	Slope morphometry	Fault scarp and offset erosional scarps
Correlative	Stratigraphy	Scarp-derived colluvial wedges
	Archaeology	Pot sherds and other artifacts
	Palynology	Offset glacial morianes
	Palaeomagnetism	Fault gouge

* method used in this thesis study

6.3 Thermoluminescence Dating

6.3.1 Basic Concept

Generally, insulators such as covalence solids and glasses can generate thermoluninescence (TL-) signal, but metals can not. As a result, TL-dating method can be only applied with an insulator crystal. A simple model to review on general background of TL-dating method is based on ionic crystal model, which is simplified as shown in Figure 6.2.

Ionic crystals, for example calcium carbonate and sodium chloride are composed of lattice of positive and negative ions. In this lattice, it can be defected due to at least three reasons; an impurity atom, a rapid cooling from the molten stage, and damage by nuclear radiation. The defected lattice is presented by lacking of electron from its proper place or electron vacancy, called electron trap, leads ionized electrons from vicinity to fill up in this trap hole. In addition, ionized electron is the result of nuclear radiation from earth materials or solar radiation. However, both nuclear radiation and solar radiation have caused much less damaged to the lattice structure.

Electrons have been trapped in trap holes lasted until shaken out due to the vibration of crystal lattice. A rapid increase of temperature to high in narrow range leads this vibration to be stronger. In addition, high temperature usually upward of 400°c can evict electrons from deep electron traps to be diffused around the crystal. Note that, because of different crystals, there are different types of traps, then optimum temperatures to evict electrons in different crystal traps are unique. However, diffused electrons can be directed into two different ways; firstly to be retrapped at different types of defect which is deeper trap, and secondly to be recombined with an ion in lattice which electrons once have previously been evicted.

According to TL-method, since it has mainly concerned only on recombination process, then the process is also reviewed in this section. Anyway, there are two types of recombination process; radiative (i.e., with light emission) or no-radiative. For this method radiative type is interested, which ions or atoms from this recombination process are called luminescence centers and the emitted light is thermoluminescence.

A simplified model of energy level to present thermoluminescence process is illustrated in Figure 6.3.

There are electron trap (T) and center of luminescence (L) located as intermediate between the valence band and the conduction band. The energy (E) is required in an optimum level to shaken out electrons from its deepest hole. In general, when electrons have already shaken out by heating, and recombination is done at the centers of luminescence, light is emitted. However, in some case which recombination has done at non-luminescence center or killer center. There is no emission of light and the energy is represented in the form of heat.

In summary, thermoluminescence process can be concluded in four steps as follows; firstly, ionization of electrons caused by nuclear radiation. Secondly, some of these electrons are trapped in continuous and constant rates lasted until temperature has incleased. Thirdly, some of electrons are heated at the optimized temperature level to evict electrons from deep trap hole. Fourthly, some of these electrons are then reach luminescence centers and in case of recombination process has done, light emission from luminescence centers is generated. The amount of emitted light or the number of photon in this stage is depended on the number of trapped electrons, which in turn is the amount of nuclear radiative proportion or paleodose. In addition, dose rate of nuclear radiative applied to environment is called annual dose.

Ultimately, based on TL-process mentioned above, age of quartz-bearing sediments (for this study) can be determined by simple equation below;

$$\text{TL-age} = \frac{\text{Paleodose}}{\text{Annual dose}} \quad \text{.....Eq. 6.1}$$

6.3.2 Paleodose and Annual Dose Evaluation

In this section, briefly descriptions on paleodose and annual dose evaluation are provided as first and second orders, respectively. Firstly, once sediment sample has been treated to become purified quartz crystals before measure their quantity of TL-intensity using TL-instrument. The apparatus diagram for TL-measurement is shown in Figure 6.4.However, due to further details of apparatus is out of scope, then it was

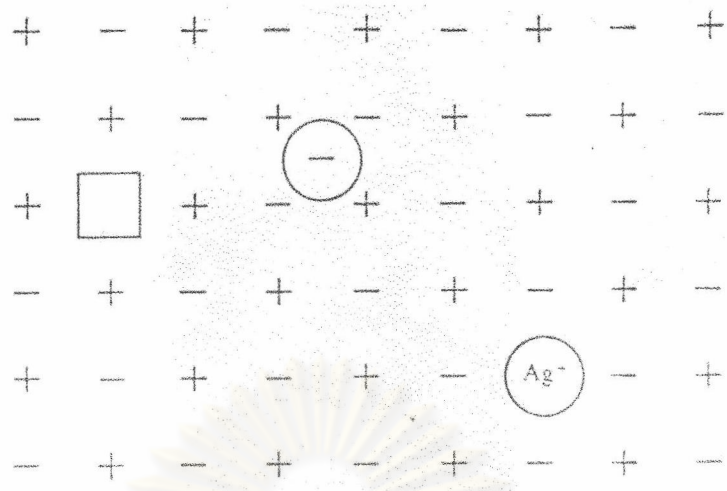

Figure 6.2. A simplified model of lattice structure of an ionic crystal showing three simple types of defect which are negative-ion vacancy on the left, negative-ion interstitial at the center, and substitutional impurity center on the bottom right (after Aitken, 1985).

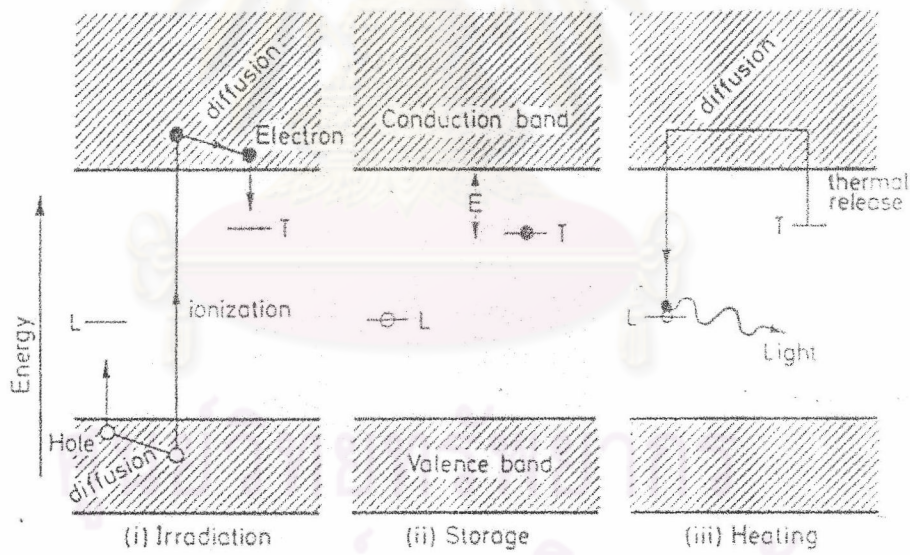

Figure 6.3. Thermoluminescence-process diagram showing energy-level related to three processes; (i) irradiation process, caused by crystal exposed to nuclear radiation, ionized electrons are trapped at hole (T). (ii) Storage stage in which electrons have been trapped, need hole deep enough for electrons (E) during geological time period of sample. (iii) Heating process, at optimum level of temperature, electrons are released and re-combined at luminescence center (L), then light (TL) is released (after Aitken, 1985).

not mention herein. The output of TL-intensity from this instrument expresses in the form of grow-curve graph as shown in Figure 6.5 in which X-axis is represented temperature and Y-axis is TL-intensity. Peak of TL-intensity in this curve is used to evaluated paleodose in the next step.

To determine paleodose, purified quartz sample has been separated into four groups; the first group is directly measured its TL-intensity called natural sample (N). The second and third have been heated to erase TL-intensity to zero before exposed to nuclear radiation environment at dose of 293 Gy and 1112 Gy, respectively. After radiation, the samples are directed to read TL-intensity. These samples are named as H+293 and H+1112. The fourth is natural sample similar to the first group, however, it is exposed to nuclear radiation at 1112 Gy before measured TL-intensity. The last sample is called natural + 1112 Gy (N+1112).

Since TL-intensity values from N, H+293, H+1112 and N+1112 have been read out, TL-ratios are then calculated. The ratios have derived from dividing all TL-intensity values by natural intensity value as follows;

TL-ratios = (1) N/N, or 1

(2) (H+293)/N

(3) (H+1112)/N

(4) (N+1112)/N

After that all of this ratio are plotted on growth-curve graph as expressed in Figure 6.6. In this graph, X-axis is represented radiation dose. Which dose of TL-ratios; (H+293)/N, (H+1112)/N, and (N+1112)/N are known as 293 Gy, 1112 Gy and more than 1112 Gy, respectively. Y-axis is represented TL-ratio. According to the curve, at the point where TL-ratio is equal to 1, paleodose of this sample can be read from this point using X-axis.

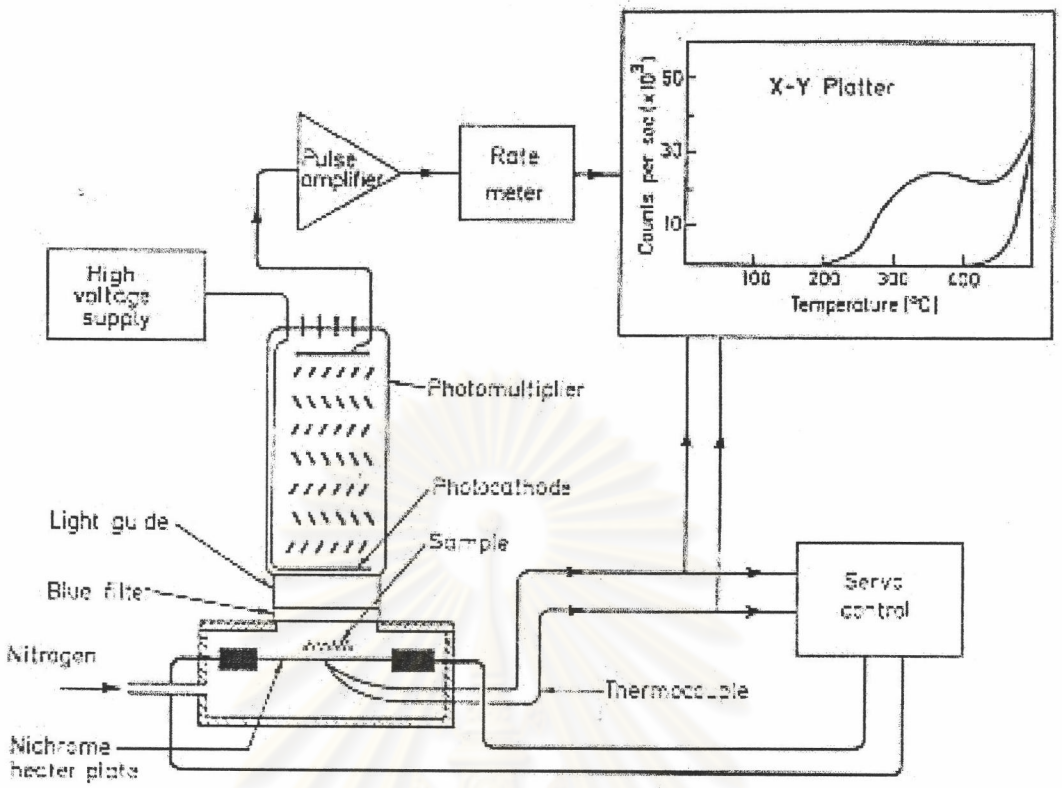

Figure 6.4. Diagram of thermoluminescence instrument (after Aitken, 1985).

Secondly, an annual dose can be derived from two main methods of investigation; in-situ and laboratory. Due to this study using only laboratory method then in-situ method was not cited herein. As general basis, annual dose is the accumulation rate of the latent thermoluminescence expressed in mGy/y. To evaluated this rate, ionization rate in the crystals, which is assumed to be equal to rate of electrons being trapped in trapped hole of crystal lattice, is needed. And in turn, this rate is the rate of energy which is generate from various radiations in natural.

In addition, depend on the conservation of energy, it is required that within the volume having dimensions greater than the ranges of the radiation, the rate of energy absorption is equal to the rate of energy emission. It can be further assumed that the matrix is uniform both in radioactivity and absorption coefficient, then the absorption of energy per unit mass is equal to the emission of energy per unit mass.

Nearly all of natural radiation are provided from potassium(K), thorium(Th) and uranium(U). However, the

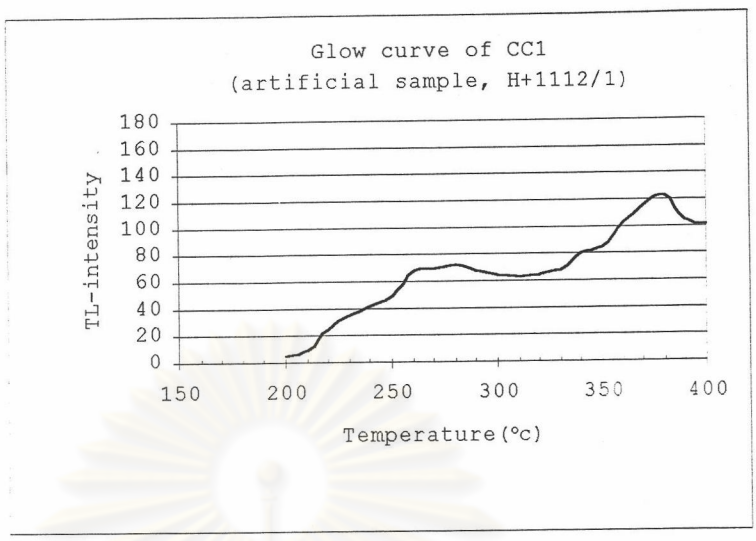

Figure 6.5. An example of glow-curve of CC1 sample which was radiative of total 1112 Gy (artificial sample) before reading its TL-intensity. Peak in this curve at 380□c is TL-intensity value.

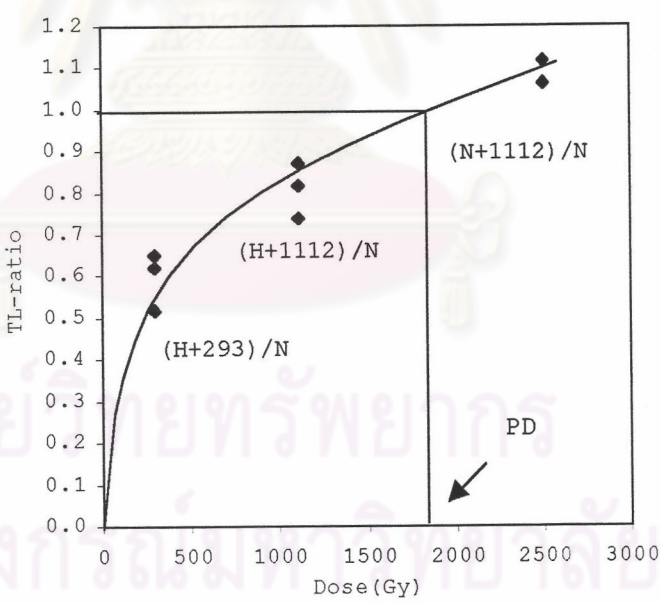

Figure 6.6. An example of growth-curve. TL-intensity of artificial samples were divided by TL-intensity of natural sample (N). Whereas natural sample intensity divided by natural intensity itself is 1 then paleodose(PD)can be acquired.

remainders which are found in a few per cent, come from rubidium and cosmic rays.

In this thesis study, X-ray spectrometer is used to measure contents of K (per cent), Th (ppm), and U (ppm) concentrated in the sample. These quantities are then calculated in order to evaluate an annual dose rate of the sample via the following equation.

$$AD = \frac{(0.1148U+0.0514Th+0.02069U)}{(1+0.14Wt)} + \frac{(0.1462U+0.0286Th+0.6893K)\beta+0.15}{(1+1.25\ Wt)}$$

.....Eq. 6.2

where;

AD = Annual dose in mGy/y
U = Quantity of uranium in ppm
Th = Quantity of Thorium in ppm
K = Quantity of potassium in form of K_2O in per cent
Wt = Water content in per cent
β = Bata absorption value which depend on grain size particle of quartz

6.3.3 Paleodose Correction

Paleodose evaluation method that has explained in the earlier section is natural paleodose [PD(Inat)]. This paleodose is composed of two values of dose accumulation. Firstly, dose which has deposited after the latest deposition of sediments and cut off sunlight, represents true paleodose of deposits. Secondly, residual paleodose [PD(Io)] which is remain stored in crystal grains of deposits prior to the latest deposition.

In conclusion;

True paleodose = PD(Inat)-PD(Io) .....Eq. 6.3

where;

PD(Inat)= Natural paleodose

PD(Io) = Residual paleodose

According to the basic concept of this correction method, it can be summarized that during crystal grain exposed to sunlight with increasing temperature, electrons are evicted with releasing paleodose in the form of TL-signals from their trapped holes to near to

zero of trapped electrons before latest deposition. After new deposition begin and cut off sunlight, ionized electrons in crystal grains, caused by radioactive, is start to re-trapped. On the other hand, time is remain in the clock caused by improper reset mode and then start to a new count, as a result time is over count in the last event.

As shown in Figure 6.7, TL glow-curves illustrated different peaks of TL-intensity read from aeolian sediments; curve(a) is the natural TL-signal, show highest peak of TL-intensity signal, curve(b) is the same sample ,but exposed to sunlight for an hour before measurement, as a result, its peak is decreased from (a), and finally curve (c) is similar to (b) however, its sample had been exposed to simulated sunlight for 24 hours before measurement, its peak is at the lowest point compared to each other.

According to this study, all sediment samples have been properly treated to become purified quartz before separated into two main groups; one for evaluating natural paleodose and another for determining residual paleodose. Natural paleodose evaluation method had already been cited in earlier section and not repeated herein. Beside, residual dose determination method is done by exposing treated sample to natural sunlight at an optimum length of time (8 hours for this study) before measure its TL-signal. When the signal has been carried out, it is then divided by natural TL-signal or N. As a result, this is a TL-ratio that ready to applied to read residual paleodose using growth-curve as shown in Figure 6.8.

Previous equation for TL-age determination is given in equation 6.1.

Depending on paledose correction method the equation of TL-age determination has been changed as following;

$$\text{TL-age} = \frac{PD(Inat)-PD(Io)}{AD} \quad \text{.....Eq.6.4}$$

where;

PD(Inat)= Natural paleodose

PD(Io) = Residual paleodose

AD = Annual dose

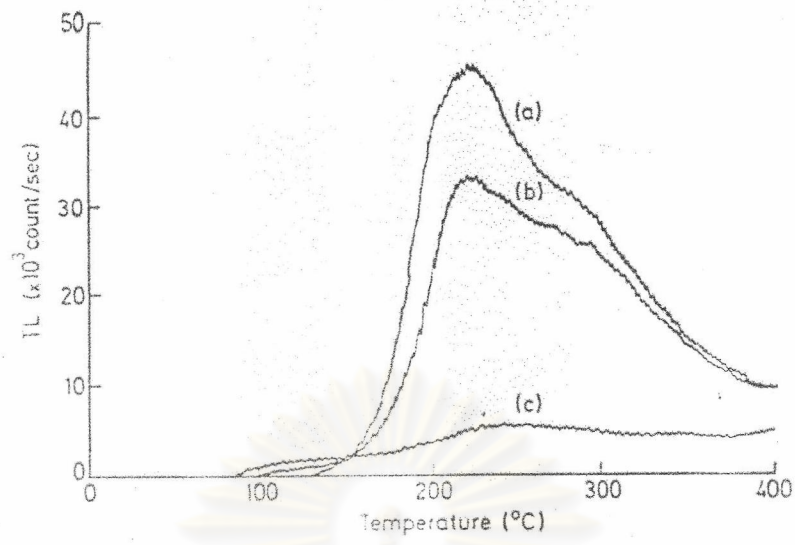

Figure 6.7. Glow-curve showing different peaks of TL-signal from beached and non-beached samples; curve (a) from non-bleached sample, curve (b) from beached sample for 1 hr exposed to sunlight and curve (c) after exposed to simulated sunlight for 24 hr (after Aitken, 1985).

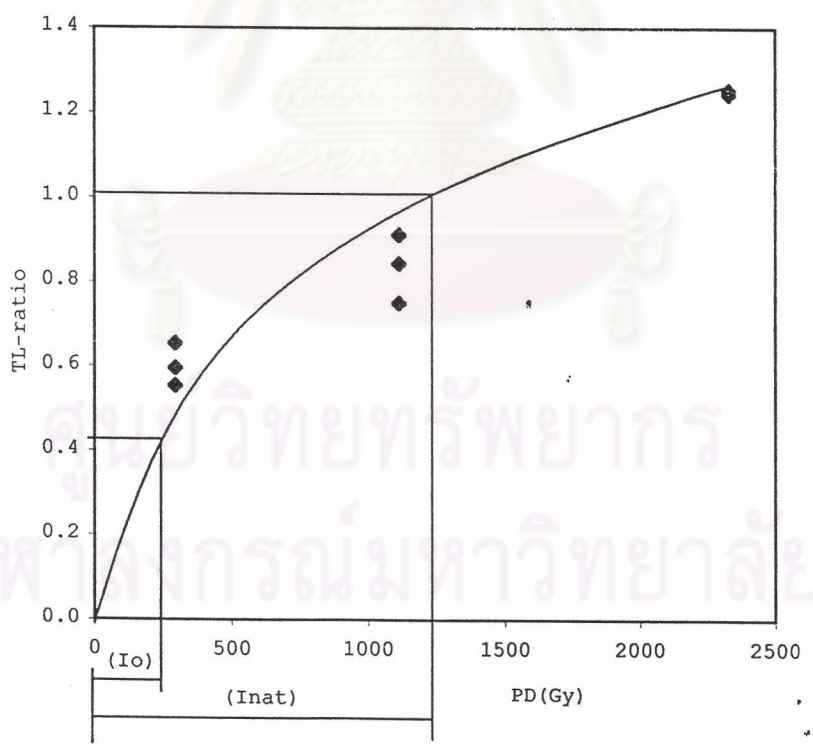

Figure 6.8. An example of growth curve. True paleodose acquires from minus natural paleodose, PD(Inat) by residual paleodose, PD(Io).

6.3.4 Plateau Test

According to glow-curve, there are overlapping peaks that may be raised to make misinterpretation of the peak, which is the result of electron emission from deep traps not other shallow traps. Glow-curve peak, which has located in the stable region, is that of interest. The stable region is usually at 300°c or higher where electrons from deep traps are evicted near to zero.

The method to recognize the stable region is plateau test as shown in Figure 6.9. There are two glow-curves of natural sample (N) and natural + artificial sample (N+β) that had been plotted as solid lines in the same graph. Ratio between N and N+β is shown as dot line. The plateau of dot line is the stable region. In addition, peaks of both samples have been generated at the same temperature, and N+β peak is higher than N peak, it means that deep traps are deep enough to contain other electrons.

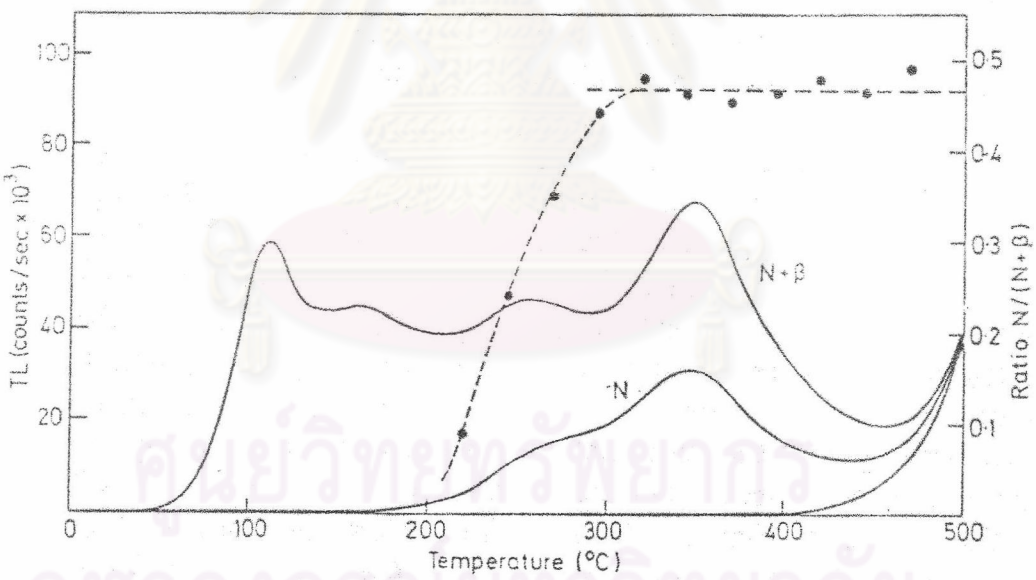

Figure 6.9. Plateau-curve (dashed line) plotted with glow-curves (solid line). Plateau-curve is the ratio of the two glow-curves; N is represented the 'natural' glow-curve and N+β is the 'natural + artificial' glow-curve (after Aitken, 1985).

6.4 TL-dating Results

Ten fault-related sediment samples had been collected from six outcrops to be used to determine their age using TL-dating method. Paleodose from almost all of samples had been corrected, excepted samples PD2-1 and PD2-2. Summarization of dating results is shown in Table 6.2. Sample details and ages are listed below.

TC sample was collected from the top layer of Ban Thung Charoen outcrop. This layer is not cut by the fault, but the lower layers are (Figure 6.10). Sediment of this top layer is reddish brown clayey gravel. TL-dating yields age 1,300,738 years or about 1,300 ka, which is the oldest sample as compared to the others.

CC1 sample from Chom-Chaeng1 outcrop was collected from the upper most faulted layer. This layer is overlain by the top layer, which shows no sign of evidence of cutting across by the fault (Figure 6.11). The sample is pale brown silty clay, yield TL-age of 175,043 years or about 170 ka. This result has shown that it is youngest age as compared to the other samples.

CC2 sample was collected from Chom-Chaeng2 outcrop nearby Chom-Chaeng1. Sampling location is located in the upper most layer. Note that all layers in this outcrop were observed cross-cut by the fault as illustrated in Figure 6.12. The sample is light brown silty clay. TL-dating has revealed the age of 831,858 years or about 830 ka.

PDL1 sample was found at the left side of Ban Pa Daeng outcrop. It was collected from the unfaulted layer as illustrated in Figure 6.13. This layer is overlain by top soil layer and underlain by faulted layers. The sample is light gray with mottle brown silty clay. TL-dating has revealed the age of 484,645 years or about 480 ka.

PDL2 sample was collected from the faulted layer underlain the unfaulted layer of PDL1 (see Figure 6.13). The sample is pale brown silty clay. TL-dating has provided the age of 1,201,368 years or about 1,200 ka.

PDR1 sampling location is sited in an unfaulted layer, which is underlain by the faulted layers and overlain by top soil layer, in the right side of Ban Pa Daeng outcrop as shown in Figure 6.14. The sample is light gray with mottle brown silty clay. TL-dating of has provided the age of 888,776 years or about 890 ka.

PDR2 sample was collected from faulted layer, which is overlain by unfaulted layer of PDR1 (see Figure 6.14). This sample is pale brown medium sand with the TL-age of 1,114,290 years or about 1,100 ka.

PD2-1 sample of pale brown sandy gravel of alluvial deposits, collected from the hangingwall of normal fault near present ground surface (Figure 6.15). TL-dating yields the age of sample 190,235 years or about 190 ka.

PD2-2 sample of pale brown silty clay, collected from the footwall of normal fault near the bottom of the outcrop (see Figure 6.15). The TL-dating result is 971,147 years or about 970 ka.

G2 sampling location is on the top layer of Garbage landfill outcrop. All layers in this outcrop were explored to be cut across by the faults (Figure 6.16). The sample is brown sandy gravel with TL-age of 613,402 years or 610 ka.

According to plateau test of all samples which are mentioned above, it is found that they reveal a stable region that has covered the glow-curve peaks. For example, the plateau test result of CC1 sample (Appendix C) show stable region (plateau) covers peaks of both natural and natural + artificial samples that means TL-signal had generated by electrons from the same deep traps.

Note that all the graphs of glow-curve, growth-curve, and plateau-test data are cited in Appendices A, B, and C, respectively.

Table 6.2. Summarization of TL-dating results.

Sample no.	Water cont.(%)	U (ppm.)	Th (ppm.)	K2O (%)	Ann. dose (mGy/y)	PD(Inat) (Gy)	PD(Io) (Gy)	PD(Inat)-PD(Io) (Gy)	TL-age (Ka.)	Error (%)
TC	16.594	1.450	4.947	0.750	1.084	1470.00	60	1410.00	1,300,738±183,924	14.14
CC1	6.570	2.913	10.089	1.271	2.308	452.00	48	404.00	175,043±25,993	14.85
CC2	15.444	2.243	9.047	1.853	2.260	2070.00	190	1880.00	831,858±242070	29.10
PDL1	12.687	2.654	8.893	1.384	2.084	1240.00	230	1010.00	484,645±102793	21.21
PDL2	4.948	2.717	8.672	1.430	2.339	3060.00	250	2810.00	1,201,368±222493	18.52
PDR1	7.982	2.190	8.370	1.230	1.969	2030.00	280	1750.00	888,776±141,226	15.89
PDR2	1.501	2.492	6.597	1.253	2.093	3275.00	880	2395.00	1,144,290±286,873	25.07
PD2-1	7.213	2.773	9.179	0.608	1.686	480.00			190,235±48,871	25.69
PD2-2	5.734	3.818	9.980	1.675	2.842	2760.00			971,147±248,631	25.60
G2	8.063	2.296	8.662	1.434	1.940	1600.00	410	1190.00	613,402±68,823	11.22

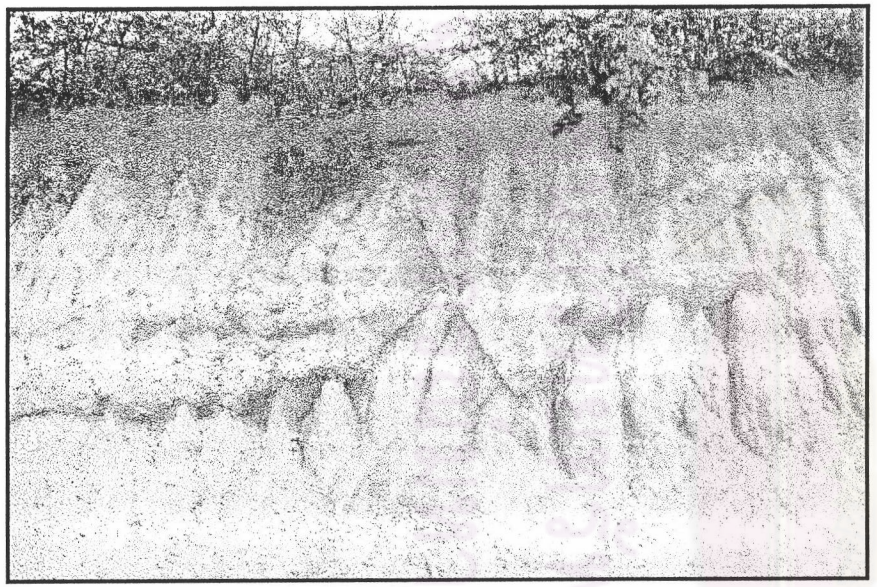

A

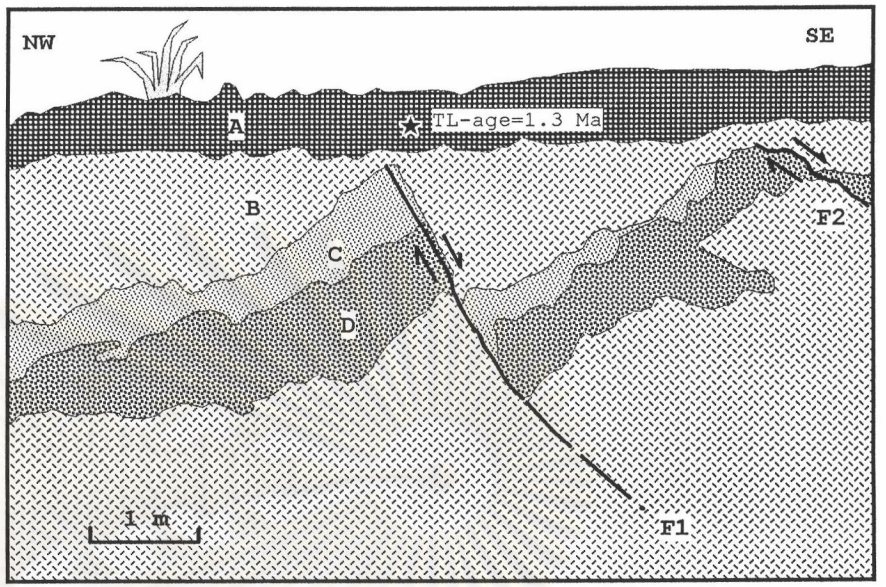

B

Figure 6.10. Thung Charoen (TC2) site (A) and outcrop logging (B). TL- age of top unit is 1.3 Ma. Faulting event occurred before this age.

Explanation

Units

- A, reddish brown gravel
- B, pale brown silty clay
- C, reddish brown sandy gravel
- D, pale brown sandy gravel

Symbols

- sampling point for dating
- contact
- observed fault with displacement
- inferred fault

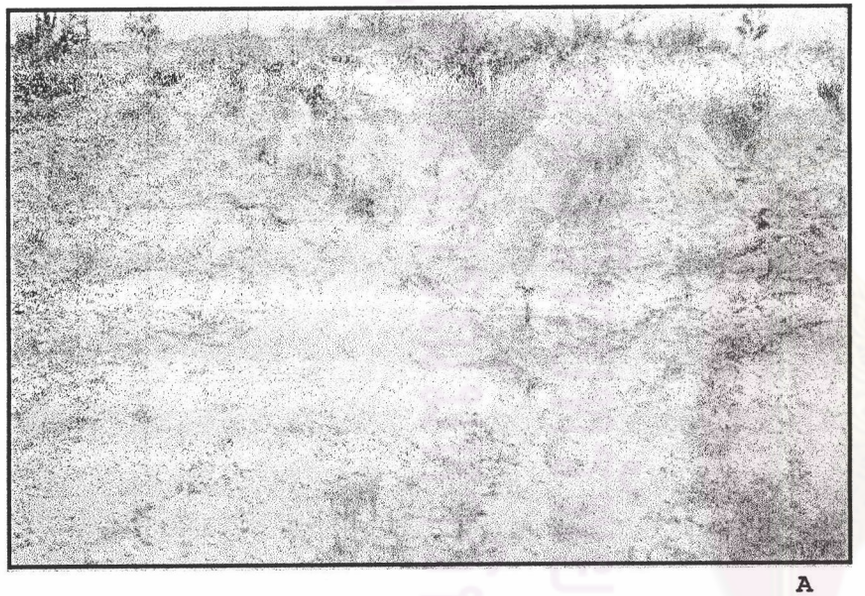

A

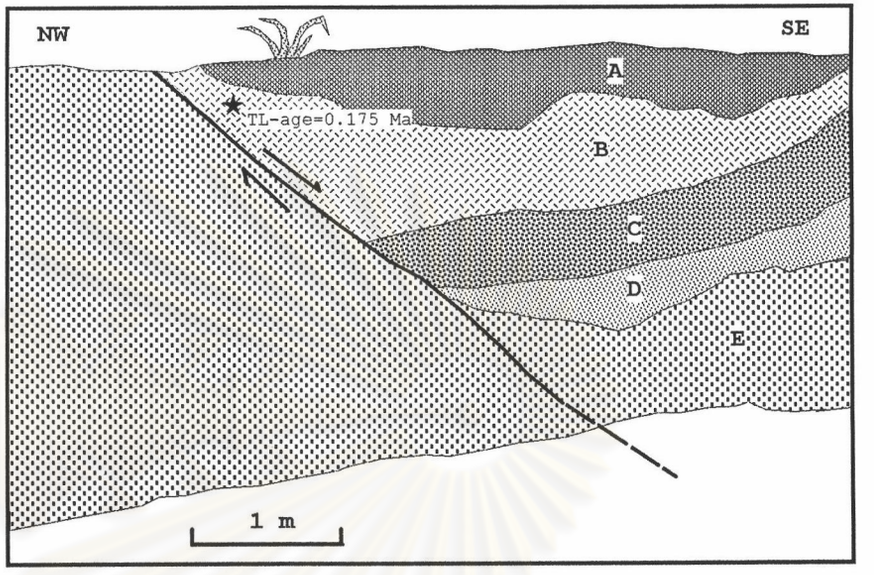

B

Explanation

Units

A, reddish brown sandy gravel

B, pale brown silty clay

C, pale brown sandy gravel

D, pale brown gravelly coarse sand

E, reddish brown sandy gravel

Symbols

sampling point for dating

contact

observed fault with displacement

inferred fault

Figure 6.11. Chom Chaeng1 (CC1) site (A) and outcrop logging (B). TL-age of unit B is 0.175 Ma. Faulting event occurred after this age.

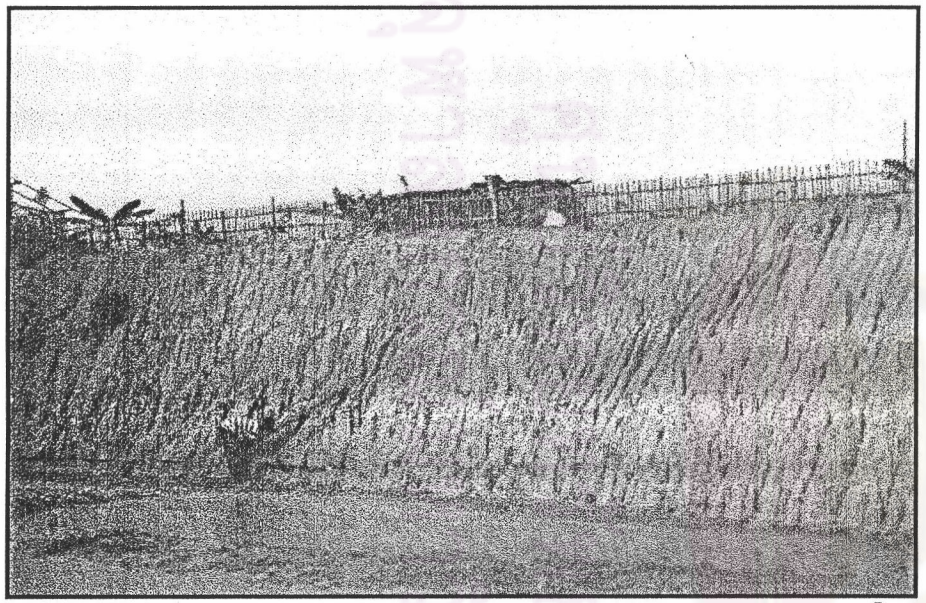

A

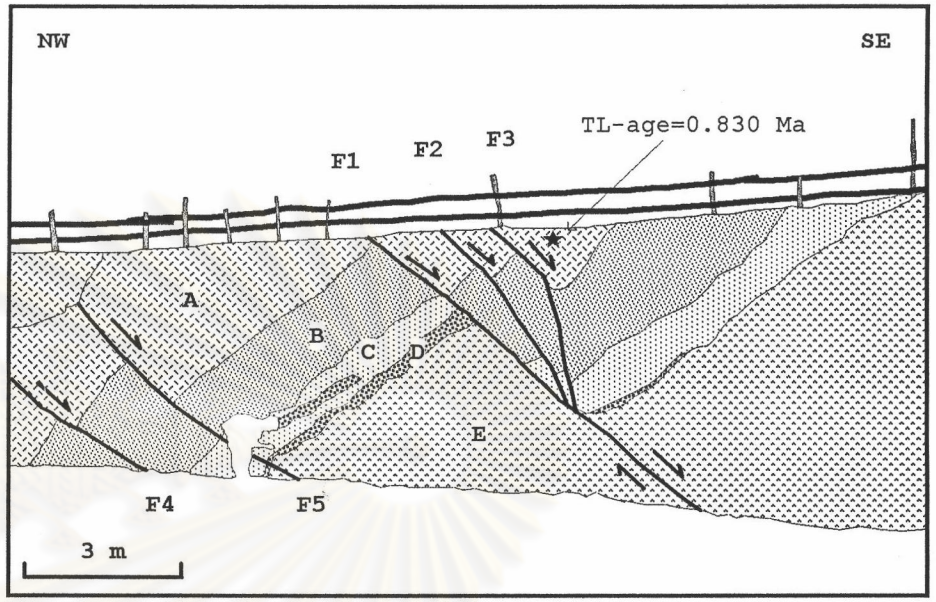

B

Figure 6.12. Chom Chaeng2 (CC2) site (A) and outcrop logging (B). TL-age of unit A is 0.830 Ma. Faulting event occurred afte this age.

Explanation

Units

- A, light brown silty clay
- B, Pale brown silty clay
- C, light gray coarse to very coarse sand
- D, light gray sandy gravel
- E, reddish brown silty clay

Symbols

- ★ sampling point for dating
- contact
- observed fault with displacement

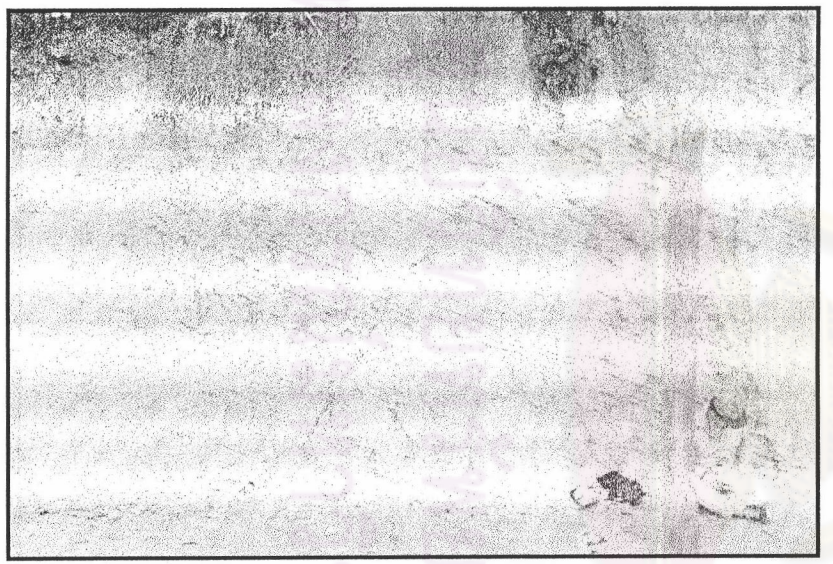

A

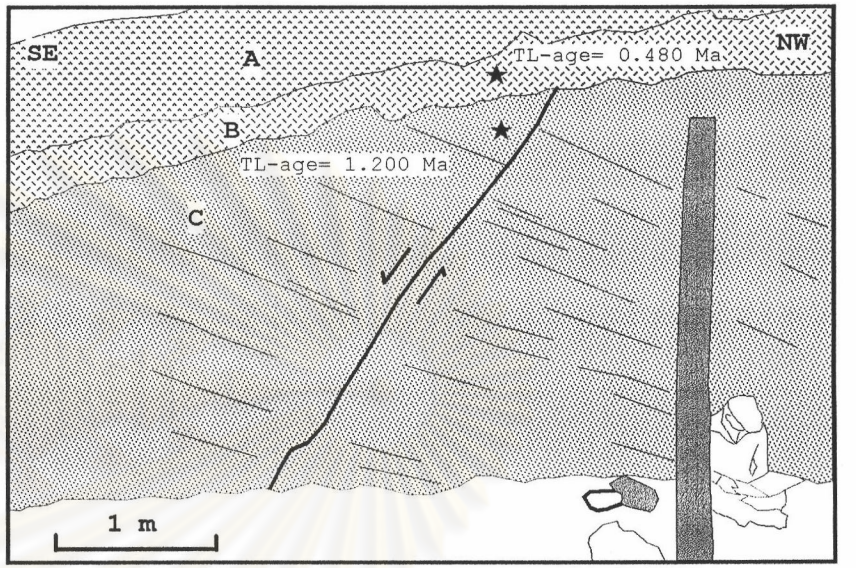

B

Figure 6.13. Pa Daeng1 (PDL) site (A) and outcrop logging (B). TL-age of unit B and Unit C are 0.480 Ma, and 1.200 Ma, respectively. Faulting event occurred between these ages.

Explanation

Units

- A, top soil
- B, light gray with mottle brown silty clay
- C, pale brown silty clay

Symbols

- sampling point for dating
- contact
- observed fault with displacement

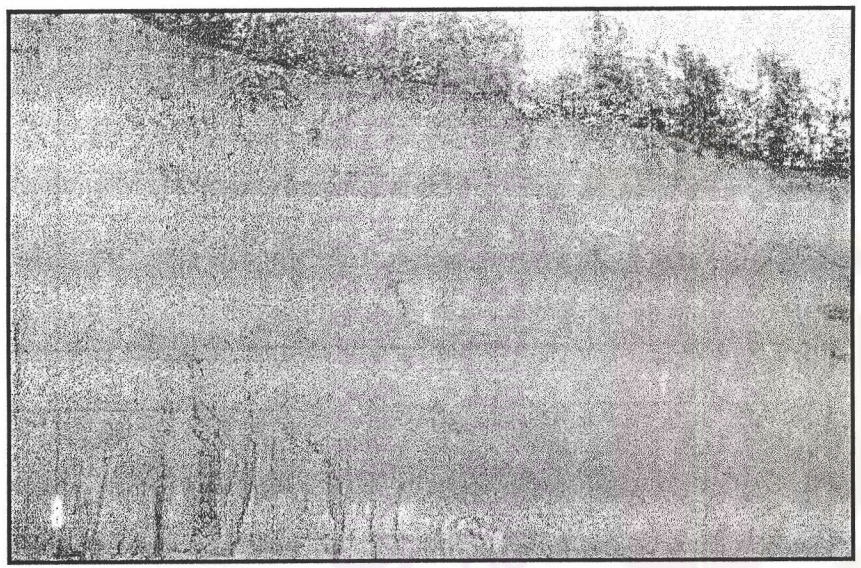

A

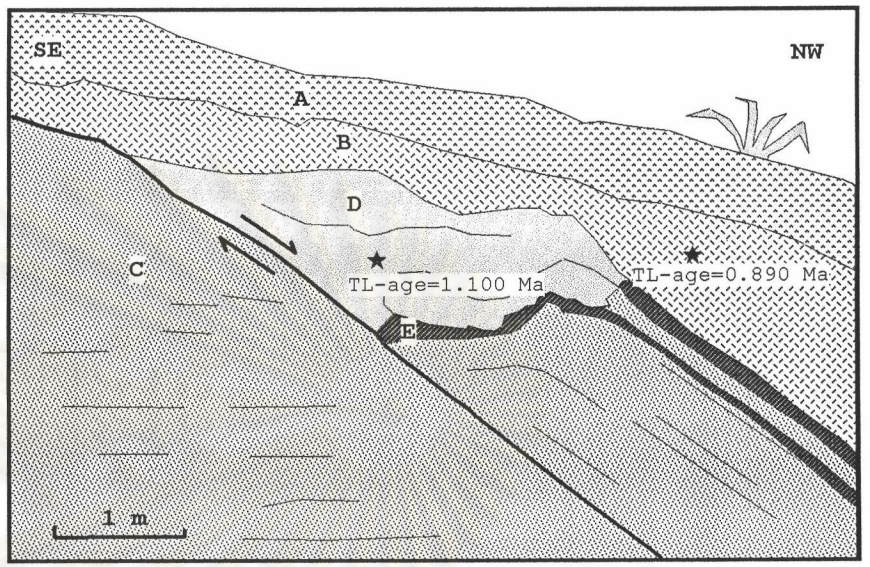

B

Figure 6.14. Pa Daeng1 (PDR) site (A) and outcrop logging (B). TL-ages of units B and D are 0.890 Ma and 1.100 Ma, respectively. Faulting event occurred between these ages.

Explanation

Units

- A, top soil
- B, light gray with mottle brown silty clay
- C, pale brown silty clay
- D, pale brown medium sand
- E, reddish brown very coarse sand

Symbols

- sampling point for dating
- contact
- observed fault with displacement

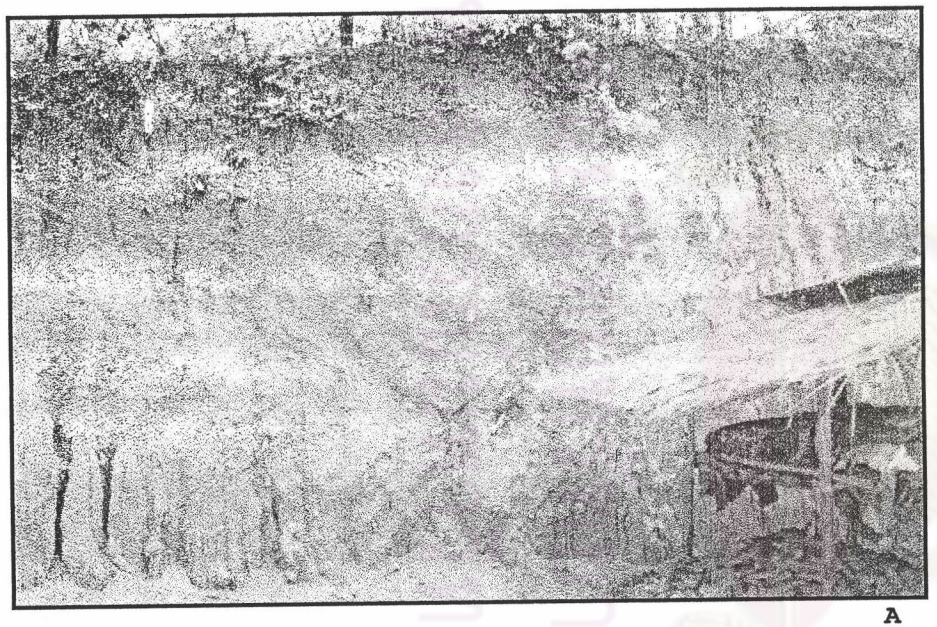

A

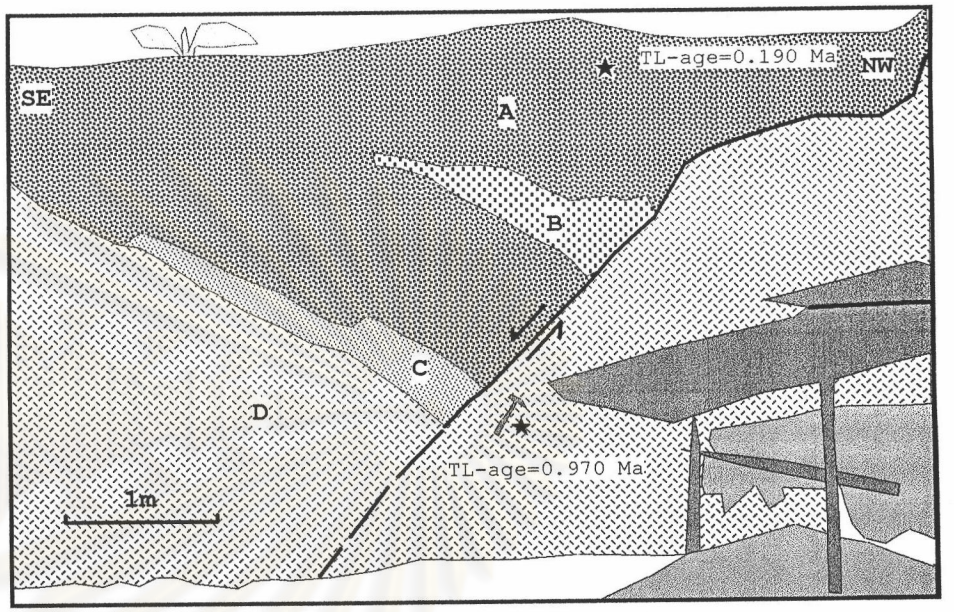

B

Figure 6.15. Pa Daeng2 (PD2) site (A) and outcrop logging(B). TL- ages of units A and D are 0.190 Ma and 0.970 Ma, respectively. Faulting event occurred after 0.190 Ma.

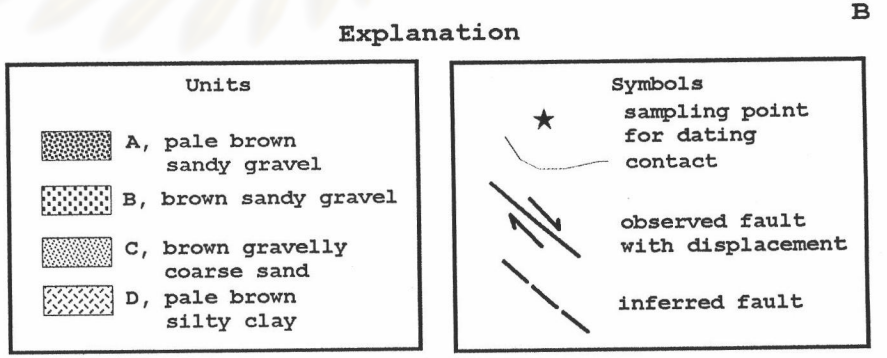

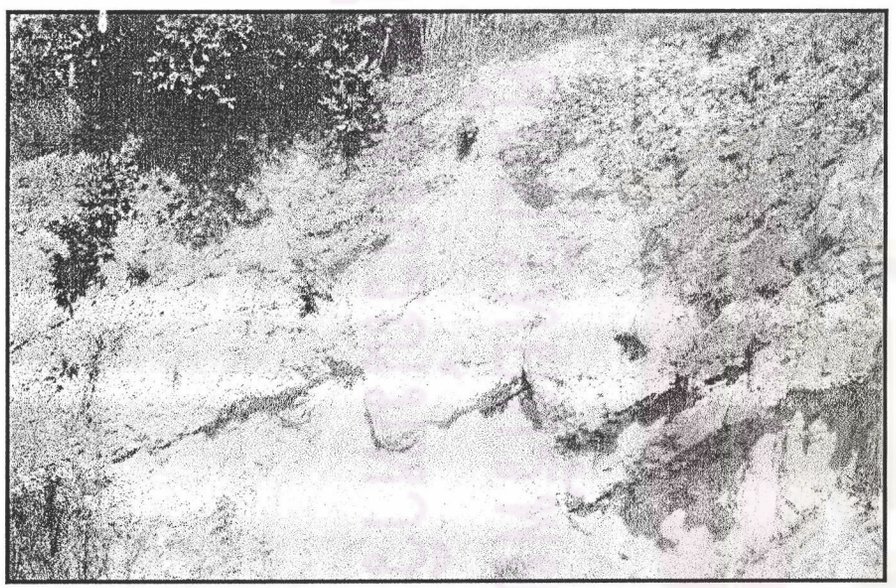

A

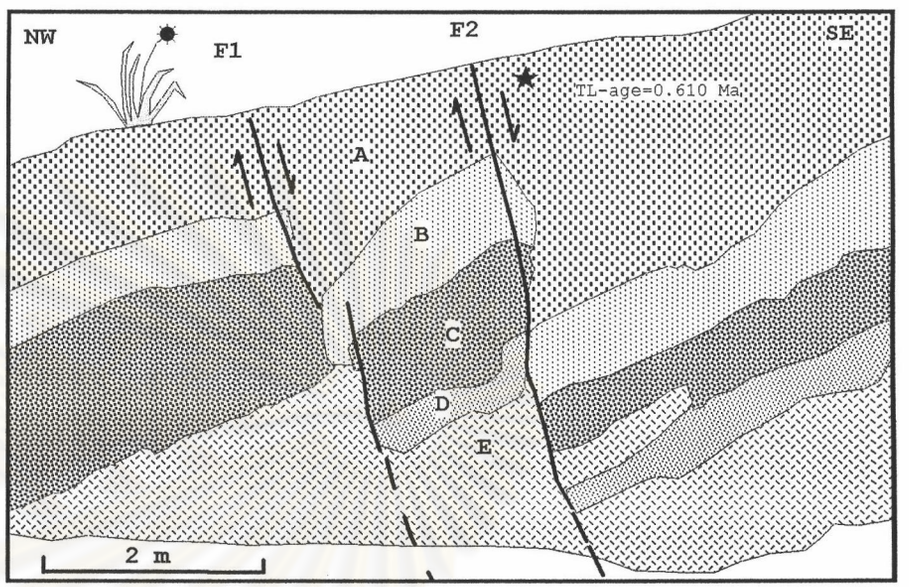

B

Figure 6.16. Garbage Lnadfill (GL) site(A) and outcrop logging(B). TL-age of unit A is 0.610 Ma. Faulting event occurred after this age.

Explanation

Units

- A, brown sandy gravel
- B, reddish brown gravelly coarse sand
- C, pale brown gravel
- D, pale brown coarse sand
- E, pale brown silty clay

Symbols

- sampling point for dating
- contact
- observed fault with displacement
- inferred fault